Polym. Bull. (2013) 70:2569–2586
DOI 10.1007/s00289-013-0972-6

ORIGINAL PAPER

Non-isothermal cold crystallization behavior and kinetics of poly(L-lactide): effect of L-lactide dimer

F. Ravari · A. Mashak · M. Nekoomanesh · H. Mobedi

Received: 7 April 2012 / Revised: 30 January 2013 / Accepted: 30 April 2013 /
Published online: 15 May 2013

Abstract The effects of L-lactide dimer as additives on the crystallization behavior of poly(L-lactide) (PLLA) films were studied. Hence, neat PLLA films and PLLA containing L-lactide (5 % w/w) (PLLA/La) were prepared in dichloromethane at room temperature via solution casting. The non-isothermal cold crystallization of PLLA films were studied using differential scanning calorimetry at various heating rates including 2.5, 5, 7.5, 10 and 15 °C/min. However, the X_C% was increased for PLLA/La films in comparison with neat PLLA films. The crystallization kinetics was then analyzed by the Avrami, Jeziorny, Ozawa and Mo kinetic models. It is found that all the kinetic models were established to describe the experimental data fairly well except the Ozawa model. The values of $t_{1/2}$, Z_C and $F(T)$ indicated that the crystallization rate increased with increase in heating rates for PLLA and PLLA/La films. However, L-lactide dimer incorporated in PLLA films accelerates the crystallization process of PLLA at the high heating rate. The nucleation constant (K_g) and the surface free energy (σ_e) based on Lauritzen–Hoffman theory indicated that these parameters for PLLA/La films is lower than neat PLLA.

Keywords Poly(L-lactide) · Crystallization kinetics · Non-isothermal cold crystallization · Differential scanning calorimetry

F. Ravari
Department of Chemistry, Payame Noor University, Tehran 19395-4697, Iran

A. Mashak · M. Nekoomanesh · H. Mobedi (✉)
Iran Polymer and Petrochemical Institute, P.O. Box: 14965/115, Tehran, Iran
e-mail: h.mobedi@ippi.ac.ir

Introduction

Poly(L-lactide) (PLLA) as a linear aliphatic thermoplastic polyester is the most favorable green polymer in various applications such as wound closure, prosthetic implants, controlled drug delivery systems and tissue engineering scaffolds due to its biodegradability and biocompatibility [1, 2]. The biodegradation characteristic of poly(L-lactide) is subject to both its crystalline morphology and crystallinity [3–5]. Therefore, it is necessary to investigate the crystallization kinetics for optimizing the process conditions and to improve the structure–property correlation. The crystallization kinetics of PLLA has been extensively studied [1, 6–10]. The melt and/or cold crystallization behavior of pure PLLA and its blends with other polymers have been studied by both isothermal and non-isothermal methods [11, 12]. Different mathematical models such as Avrami, Jeziorny, Ozawa and Mo were used to explain the crystallization process. Liu et al. [1] had compared the crystallization kinetics of pure PLLA with poly(L-lactide) stereocopolymer (PL_{98}) containing 98 % L-lactyl and 2 % D-lactyl units using differential scanning calorimetry (DSC). Ohtani et al. [13] had studied a mechanism of phase transformation for the cold crystallization of PLLA. They showed that the crystallinity of PLLA is controlled by its composition. Schmidt et al. [14] indicated that the overall crystallization extent of PLLA was reduced in the presence of poly(D-lactide) (PDLA). Baratian et al. [15] found that the crystallinity and spherulite growth decreased with increase in the content of D-lactide in PLLA. PLLA has a crystallization rate slower than commercial thermoplastics. Using of nucleating agent is the most practicable method to enhance the overall crystallization rate. Hydroxyapatite [16], montmorillonite [17], silicon dioxide [18], starch and its derivatives [19], aliphatic amide [20], and carbon nanotubes [21, 22] were added into the PLLA matrix as nucleating agent. However, some of these materials improve mechanical properties of the polymer matrix [23].

Recently we reported on the degradation and crystallization behavior of PLLA in the presence of L-lactide dimer candidate for medical, pharmaceutical and packaging applications [24, 25]. Since the degradation rate of PLLA was influenced by polymer crystallinity, the objective of the study reported in the present paper was to investigate the non-isothermal crystallization kinetics of PLLA containing L-lactide dimer. Various mathematical models, i.e., Avrami, Jeziorny, Ozawa and Mo models are applied to deal with the experimental data obtained using the DSC technique. Also, the crystallization kinetics of polymeric films has been analyzed using the Lauritzen–Hoffman equation.

Experimental

Materials

PLLA (RESOMER L 210) with an inherent viscosity of 3.3–4.3 dL/g (0.1 % in chloroform) and L-lactide were purchased from Boehringer Ingelheim Pharma GmbH & Co. (KG, Germany). L-Lactide was recrystallized from ethyl acetate and

dried at room temperature for 48 h. Dichloromethane, ethyl acetate and methanol were provided by Merck (Germany).

PLLA and PLLA/La film preparation

The PLLA films were prepared by a solvent casting method. Poly(L-lactide) powder was dissolved in dichloromethane and L-lactide dimer (5 % w/w) was added. The PLLA solution was poured into a flat dish to evaporate the solvent at room temperature for 24 h. The samples were further dried at 50 °C for 3 days to remove the solvent completely. The thicknesses of polymer films were about 100–150 μm. The solubility of L-lactide in dichloromethane was supposed to be perfect within L-lactide concentration studied since no phase separation was observed.

Measurements

The crystallization studies were carried out by DSC (Polylabe 625, instrument, UK). The film samples were about 5 mg in weight throughout the experiments. The samples were heated from room temperature to 230 °C at 10 °C/min and held for 5 min to eliminate the previous thermal history. Then, the samples were cooled to 20 °C at the rate of 10 °C/min and again heated to 230 °C at the predetermined rates consequent. The non-isothermal process includes cold crystallization at different heating rates: 2.5, 5, 7.5, 10 and 15 °C/min. The exothermal curves of heat flow were recorded as a function of temperature. The experiments were carried out under nitrogen.

The change in weight of the PLLA films due to possible decomposition was determined using a thermogravimetric analyzer (DSC/TGA 1, Mettler Toledo). Thermogravimetric analysis (TGA) data for PLLA films were taken at a rate of 20 °C/min in nitrogen atmosphere.

Results and discussion

DSC offers a fast method for studying polymer crystallinity upon the heat required to melt the polymer. It is well known that the crystalline polymers such as polylactide are able to crystallize between glass transition temperature, T_g, and melting point temperature, T_m. The crystallization process can be classified into two categories. If the initial state was the molten state, it is called melt crystallization. In cold crystallization, the initial state is the amorphous state and the samples should be kept at a temperature lower than its T_g [23]. In this paper, crystallization behaviors of PLLA matrices from their amorphous state were studied.

Non-isothermal crystallization behavior

Thermal stability of PLLA film was investigated by a thermogravimetric analyzer from room temperature to 700 °C with heating rates 20 °C/min under nitrogen atmosphere. Weight loss/temperature curves were recorded (Fig. 1). The plot shows

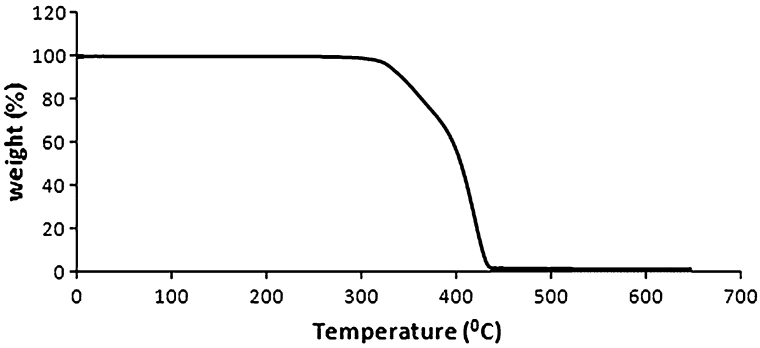

Fig. 1 TGA thermogram of PLLA

that PLLA film undergoes thermal degradation beginning at 300 °C. The results confirm that PLLA is thermally stable under non-isothermal condition studied.

The information from the total DSC thermograms for neat PLLA and PLLA/La films (Fig. 2) reflects no remarkable exothermic events during the cooling process of melt samples at the cooling rate of 10 °C/min. These results indicate that the PLLA samples almost have an amorphous structure at beginning of the second heating process.

The thermograms of neat PLLA and PLLA containing L-lactide (5 % w/w) (PLLA/La) for second heating scan at various heating rates are shown in Fig. 3. The curves show an exothermic cold crystallization peak, at about 88–122 °C for neat PLLA films and at 72–91 °C for PLLA/La samples, and also an endothermic peak related to melting at about 172–179 °C for neat PLLA and at 162–165 °C for PLLA/La films. Clearly, crystallization temperatures (T_C) shift gradually to the higher temperatures with increasing heat rates for both samples. It indicates that the chains need more time for crystallization at higher heating rate. Also, it could be related to lower heat transfer coefficient of the polymers which delay crystallization with increasing heating rate. Another finding is that the L-lactide-filled PLLA films show lower T_C compared with neat PLLA samples. It suggests that the presence of L-lactide can promote initial cold crystallization of PLLA films due to the heterogeneous nucleation effect which offers more sites for nucleation and accelerates the deposition of polymer molecules.

The data obtained from Fig. 3 are listed in Table 1. T_C is the temperature of cold crystallization peak and ΔH_C is the enthalpy of cold crystallization normalized to unit mass of PLLA matrix. The degree of crystallinity of the samples, X_C% obtained from the melting enthalpy of the polymers was compared to that of perfect PLLA crystals (95 J g^{-1}) [26]. W_p is introduced as the weight fraction of the polymer matrix.

The results show that X_C% was increased for PLLA/La films in comparison with neat PLLA films.

The relative degree of crystallinity, $X(t)$ as a function of the crystallization temperature or time is determined from the crystallization exotherms of polymers by

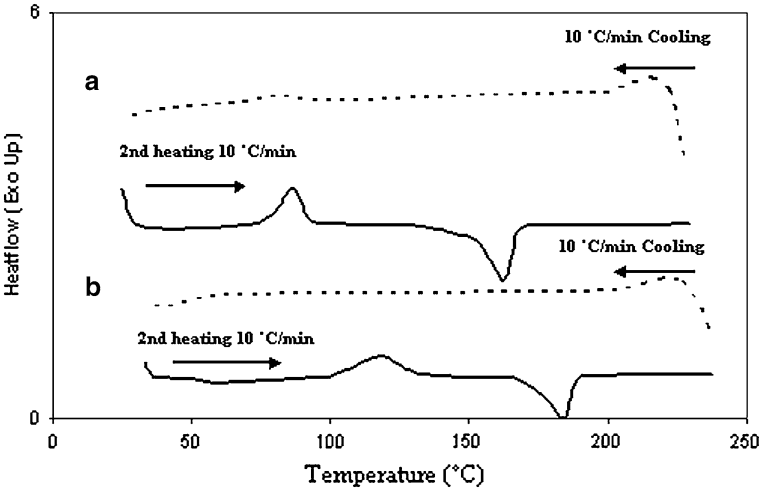

Fig. 2 DSC thermograms of PLLA/La (**a**) and neat PLLA (**b**) films

partial integration of the crystallization exotherms. $X(t)$ as a function of the temperature can be defined by Eq. (1):

$$X(t) = \frac{\int_{T_0}^{T} \left(\frac{dH_C}{dT}\right) dT}{\int_{T_0}^{T_\infty} \left(\frac{dH_C}{dT}\right) dT} \quad (1)$$

where T_0 and T_∞ are the onset and end of crystallization temperatures, respectively.

For the non-isothermal cold crystallization process, the relationship between crystallization time, t and the corresponding temperature, T can be signified as follows:

$$t = \frac{T - T_0}{\phi} \quad (2)$$

where ϕ is the heating rate [27]. Figure 4 shows the variation of relative crystallinity with crystallization time for neat PLLA and PLLA/La. All these curves at various heating rates have the same characteristic of sigmoidal shape due to the spherulite impingement in the later stage of crystallization. This would indicate that only the lag effects of heating rates on crystallization were observed for these curves. The figures also show that at higher heating rates, PLLA matrices have shorter time of crystallization which meant that the crystallization rates were increased. Similar results have also been reported by Wu et al. [28] for non-isothermal cold crystallization of PLLA.

From Fig. 4, it is clear that the relative degree of crystallinity for PLLA matrix containing L-lactide occurs at lower times in comparison with neat PLLA films.

The half-time of crystallization ($t_{1/2}$) is an important parameter for investigation of crystallization kinetics. The time required to reach 50 % crystallization is called

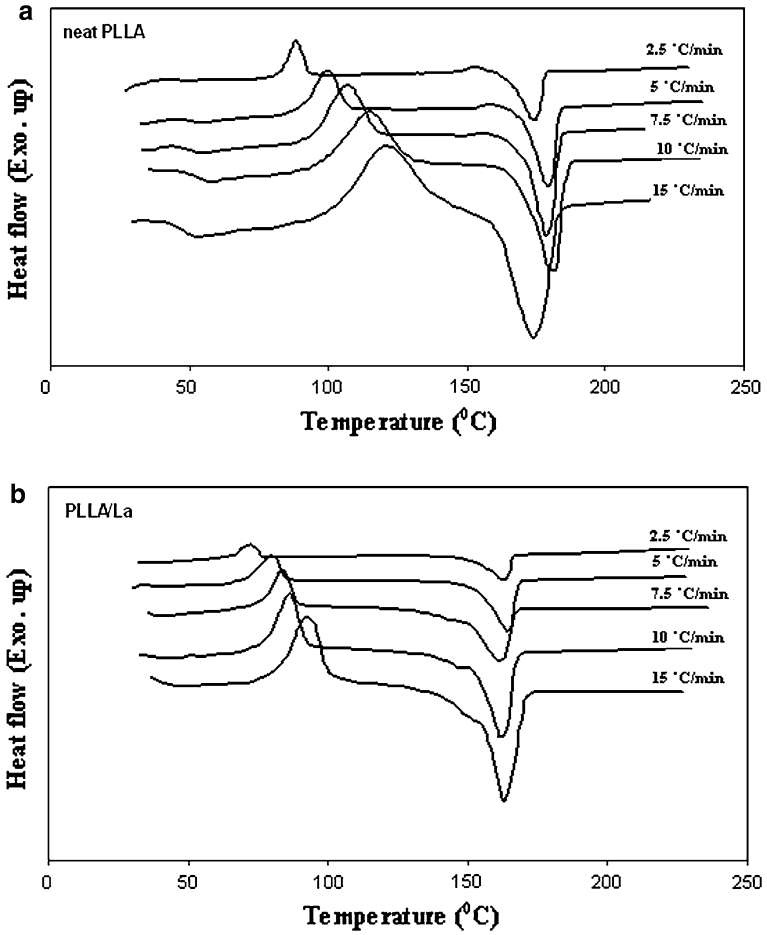

Fig. 3 The thermograms of neat PLLA (**a**) and PLLA/La (**b**) during non-isothermal crystallization at various heating rates

half-time of crystallization. The $t_{1/2}$ of non-isothermal crystallization can be obtained from Fig. 4 and can be used to discuss the non-isothermal crystallization rates. The data are shown in Table 2. Generally, if $t_{1/2}$ is short, then the crystallization is fast. The $t_{1/2}$ values indicate that the higher heating rates have shorter crystallization completion times for both neat PLLA and PLLA/La. Moreover, the values of $t_{1/2}$ for PLLA/La films are lower in comparison to those of neat PLLA films at higher heating rates. It can be suggested that in comparison with neat PLLA, the incorporation of L-lactide dimer accelerates the overall cold crystallization process. However, higher $t_{1/2}$ values for these films at lower heating rates ($\leq$5 °C/min) may be attributed to second crystallization process.

Table 1 The data obtained from the DSC thermograms of neat PLLA and PLLA/La

Sample	φ (°C/min)	T_C	ΔH_C	T_m	$-\Delta H_m$	X_C (%)
PLLA	2.5	88.7	30.84	174.5	63.65	67
	5	101.1	33.18	179.8	49.25	51.8
	7.5	107.6	37.17	177.8	43.34	45.6
	10	114.6	38.48	179.1	40.72	42.8
	15	122.1	37.8	174.7	43.37	45.6
PLLA/La	2.5	72.4	23.16	163.5	55.39	61.3
	5	80.4	29	165.4	52	57.6
	7.5	84.3	22.84	163	50.6	56
	10	87.1	34.22	162.2	57.1	63.2
	15	91.2	35.36	163	53.5	59.2

$X_C\% = (\Delta H_m/(95 \times W_p)) \times 100$

Non-isothermal crystallization kinetic analysis

Analysis based on the Avrami theory

Several methods have been developed to consider the kinetic parameters of non-isothermal crystallization. The Avrami equation has been adapted to describe the crystallization process in polymers [29]. It is used to analyze the increase of relative crystallinity with time:

$$X(t) = 1 - \exp(-kt^n) \tag{3}$$

$$\log[-\ln(1 - X(t))] = \log k + n \log t \tag{4}$$

where k and n are the crystallization rate constant and Avrami exponent, respectively. These kinetic parameters denote that crystallization mechanism constants depend on the type of nucleation (homogeneous or heterogeneous) and the growth dimension [1].

The Avrami exponent (n) and crystallization rate constant (k) can be obtained by plotting $\log[-\ln(1 - X(t))]$ as a function of $\log t$, as shown in Fig. 5.

All the related crystallization kinetic parameters from Avrami model are listed in Table 2. The obtained Avrami exponents, n for neat PLLA and PLLA/La films were in the range of 3.2–4.3. The values of n reported in literatures for PLLA were in the range of 2–5.4. These values depend on the mechanism of nucleation, the form of crystal growth and the detecting techniques used [30]. It is well known that the parameter of Avrami exponent, n describes the growing mechanism and geometry of crystallization. The calculated Avrami exponents for neat PLLA and PLLA/La films are in accordance with that reported in the literatures [14, 28], suggesting a spherulite growth and random nucleation.

In addition, slight difference in average values of n indicates that crystallization mechanism of PLLA films may not alter during temperature variation of the crystallization. Avrami plots generally deviate from the linear regression at a higher

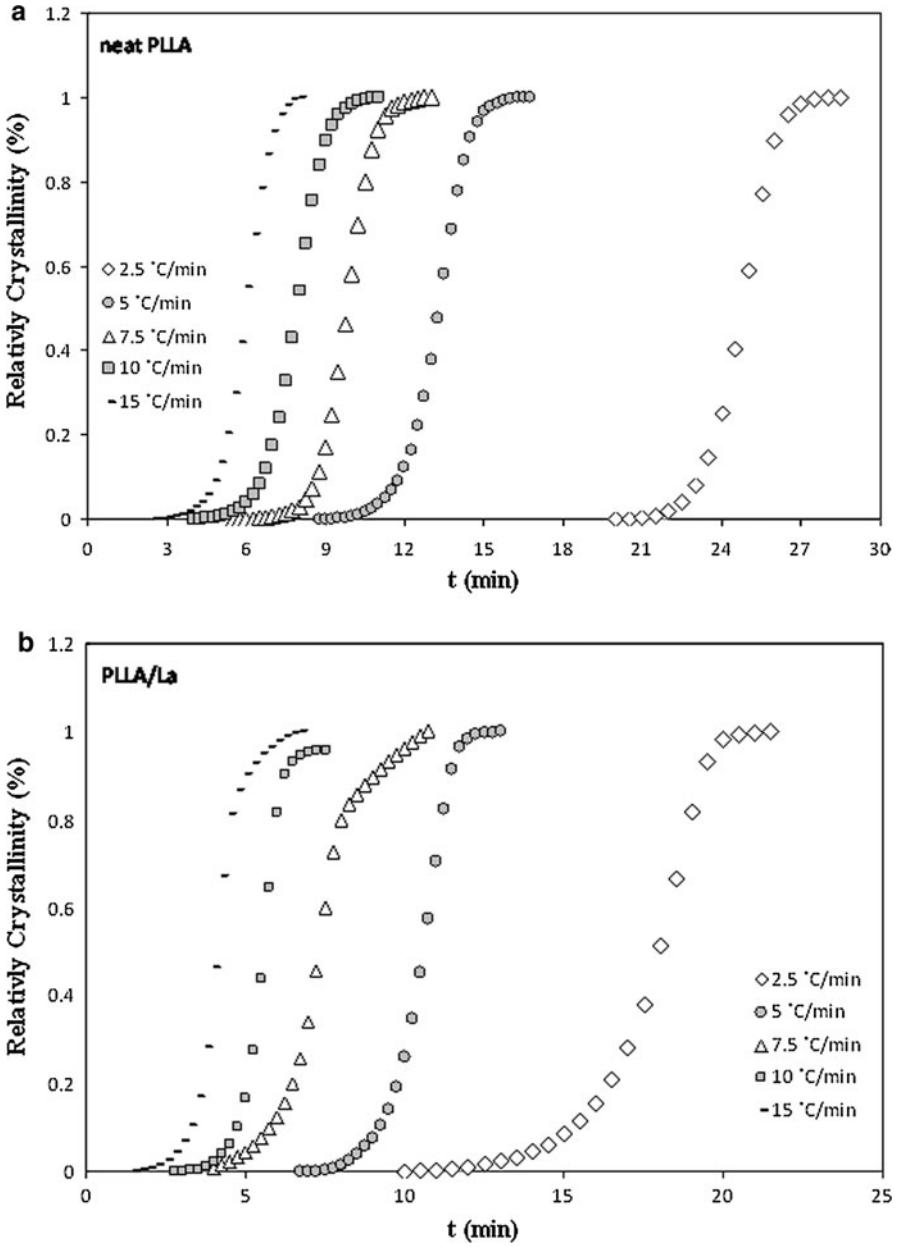

Fig. 4 Relative crystallinity versus time for neat PLLA (**a**) and PLLA/La (**b**) at various heating rates

crystallization ratio mainly due to ignoring the considerable role of secondary crystallization process [1].

The temperature changes constantly during non-isothermal crystallization, hence the parameters n and k have different physical meanings. Therefore, Jeziorny

Table 2 The data from Avrami and Jeziorny models

Sample	φ (°C/min)	$t_{1/2}$ (min)	Log k	n	Z_C
PLLA	2.5	4.8	−2.82	3.8	0.07
	5	4.6	−2.74	3.8	0.28
	7.5	4.7	−2.669	3.7	0.44
	10	4.0	−2.341	3.5	0.58
	15	3.7	−2.034	3.2	0.73
				3.6 (average)	
PLLA/La	2.5	8.6	−3.64	3.7	0.03
	5	5.2	−3.273	4.3	0.22
	7.5	3.9	−2.437	3.8	0.47
	10	2.9	−2.063	4	0.62
	15	2.8	−1.615	3.2	0.78
				3.8 (average)	

considered correcting the crystallization rate constants by introducing heating rate. The modified equation is expressed by Eq. (5) [31]:

$$\log Z_C = \frac{\log Z_t}{\phi} \tag{5}$$

where Z_C is the modified crystallization rate constant and Z_t is the rate constant in the non-isothermal crystallization process.

The values of Z_C are shown in Table 2. The modified crystallization rate constant of additive loaded PLLA films increases to some extent in contrast to that of neat PLLA at the heating rate more than 5 °C/min. Since Z_C parameter describes the growth rates of the crystals under non-isothermal crystallization process, these results show that L-lactide dimer can accelerate the cold crystallization process, which was also reflected by the decrease in the half crystallization time ($t_{1/2}$) at high heating rate. However, at the low heating rates <5 °C/min, Z_C value of L-lactide-loaded PLLA are smaller than neat PLLA. It may be due to the slower growth rates of the crystals.

Analysis based on the Ozawa method

The Ozawa model is one of the most used kinetic approaches for the crystallization process in which the Avrami equation is extended [32]. It assumes that the non-isothermal crystallization process is divided into small isothermal steps. The Ozawa equation is expressed by Eq. (6):

$$X(t) = 1 - \exp\left[\frac{-K(T)}{\phi^m}\right] \tag{6}$$

$$\ln[-\ln(1 - X(t))] = \ln K(T) - m \ln \phi \tag{7}$$

where $K(T)$ and m are the heating function and the Ozawa exponent, respectively. Ozawa exponent depends on the dimension of crystal growth. Plots of

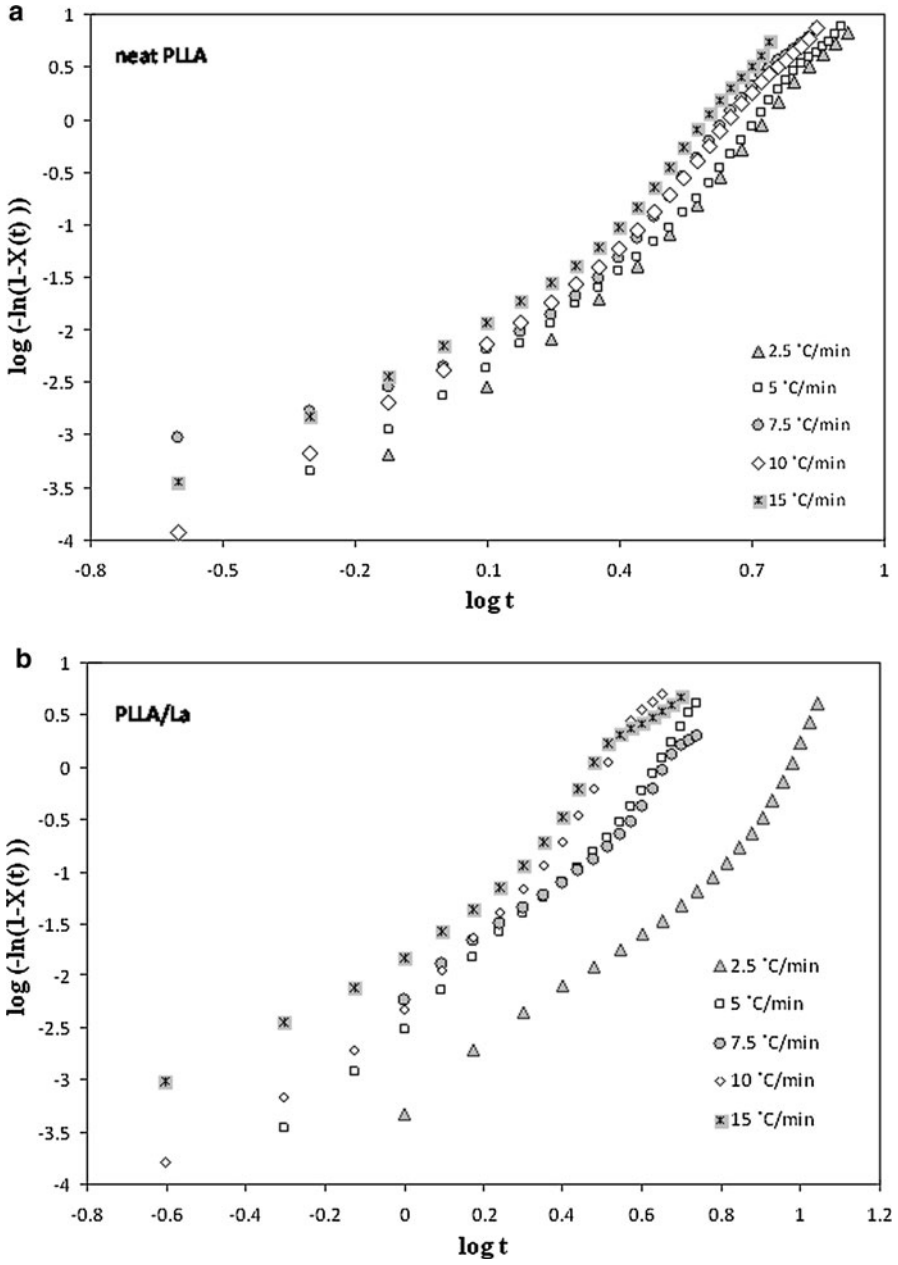

Fig. 5 Avrami plots of $\log[-\ln(1-X(t))]$ versus $\log t$ for neat PLLA (**a**) and PLLA/La (**b**) films

$\ln[-\ln(1-X(t))]$ versus $\ln\phi$ are shown in Fig. 6 and are used for obtaining the Ozawa kinetic parameters.

It can be seen that these figures have shown some curvature. These changing slopes indicate that m is not constant with temperature. Thus, the Ozawa method is

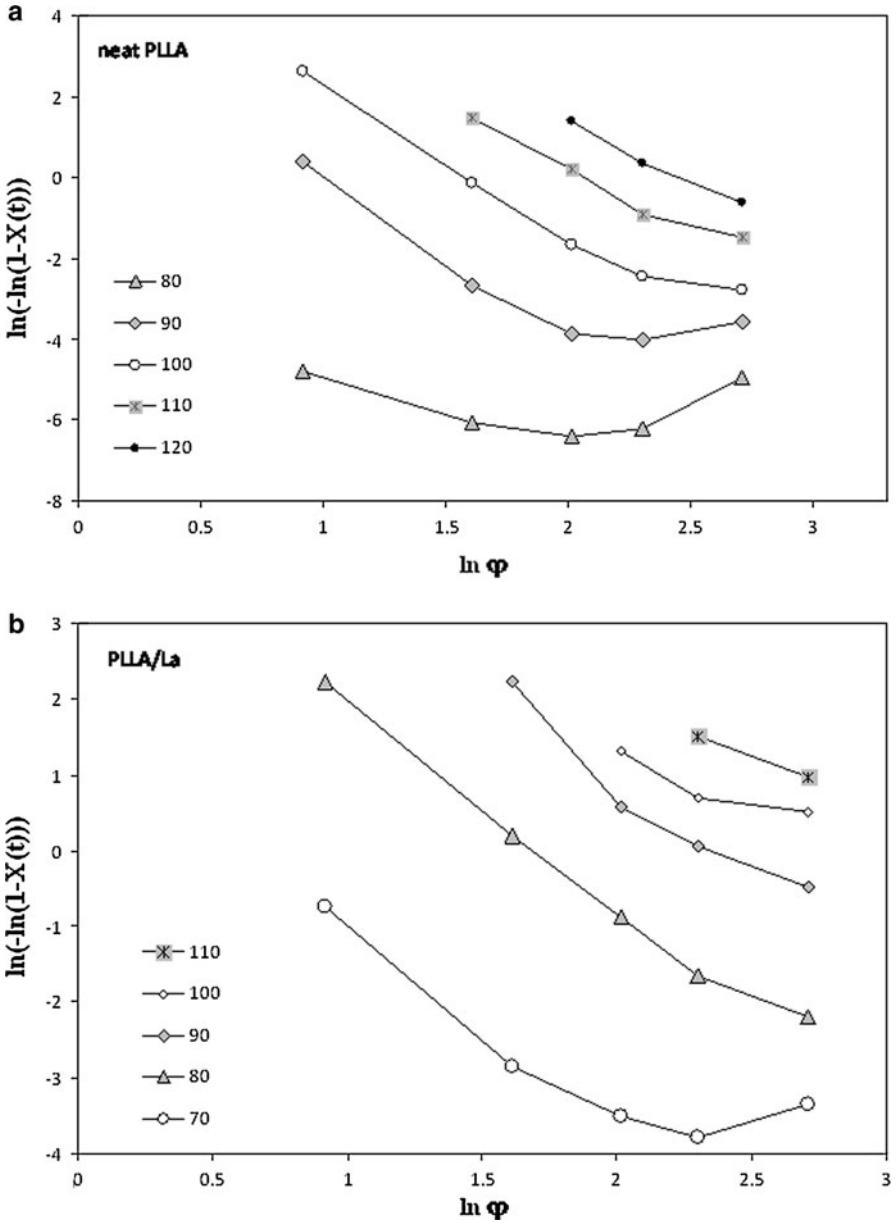

Fig. 6 The Ozawa plots of neat PLLA (**a**) and PLLA/La (**b**) films

not satisfactory to describe the cold crystallization kinetics of neat PLLA and PLLA/La films. Some authors have declared that the Ozawa model cannot be applied for modeling the crystallization kinetics of polymers that have secondary crystallization. Similar results were also found for neat PLLA and its blends [23, 28].

Combined Avrami and Ozawa equations

Mo and coworkers [33, 34] have suggested a new method to explain the non-isothermal crystallization process. This method is a combination of the Avrami and Ozawa equations at a given value of $X(t)$ as follows:

$$\ln \phi = \ln F(T) - \alpha \ln t \tag{8}$$

where $F(T) = [K(T)/Z_t]^{1/m}$ refers to the value of heating rate and α is the ratio of n to m. Plots of $\ln \phi$ versus $\ln t$ yield a linear relationship for a certain relative degree of crystallinity, as shown in Fig. 7.

It can be seen that the Mo model is successful in describing the non-isothermal process of PLLA and PLLA/La films. The values of α and $F(T)$ can be calculated from the slope and the intercept of the lines. The details of kinetic parameters are listed in Table 3.

The values of α are from 2.05 to 2.41 for neat PLLA and from 1.48 to 1.67 for PLLA/La films. The data show that the values of $F(T)$ increased with the increasing relative crystallinity. On the other hands, neat PLLA revealed a higher $F(T)$ values compared to the values achieved for PLLA/La at the same $X(t)$ values. Since $F(T)$ reflects the difficulty of crystallization process, it is determined that at the similar $X(t)$ values, the smaller $F(T)$ values for L-lactide-loaded PLLA film is in agreement with faster crystallization rates. This is also in agreement with other kinetic parameters (such as $t_{1/2}$ and Z_C).

Crystallization activation energy of PLLA films

The crystallization activation energy, ΔE, for non-isothermal cold crystallization of neat PLLA and PLLA/La films was estimated from the Kissinger method. This method is applied to determine ΔE for the transport of the polymer segments to the growing surface, by calculating the variation of T_C with the heating rate (ϕ) [35]:

$$\frac{d\left[\ln\left(\frac{\phi}{T_C^2}\right)\right]}{d\left(\frac{1}{T_C}\right)} = -\frac{\Delta E}{R} \tag{9}$$

where ΔE is the activation energy, T_C the crystallization peak temperature, and R is the universal gas constant. ΔE can be obtained from the slope of plots of $\ln\left(\frac{\phi}{T_C^2}\right)$ versus $\frac{1}{T_C}$ (Fig. 8).

The ΔE values from Fig. 8 were calculated to be 55.7 and 92.4 kJ mol^{-1} for neat PLLA and PLLA/La films, respectively. It is clear that the cold crystallization activation energy of the L-lactide loaded PLLA films is higher than that of neat PLLA. Similar results have also been found for the cold crystallization activation energy of PLLA in the presence of the multiwalled carbon nanotubes [23] and clay [28], in which for both mixtures the addition of additive unexpectedly increased the ΔE values.

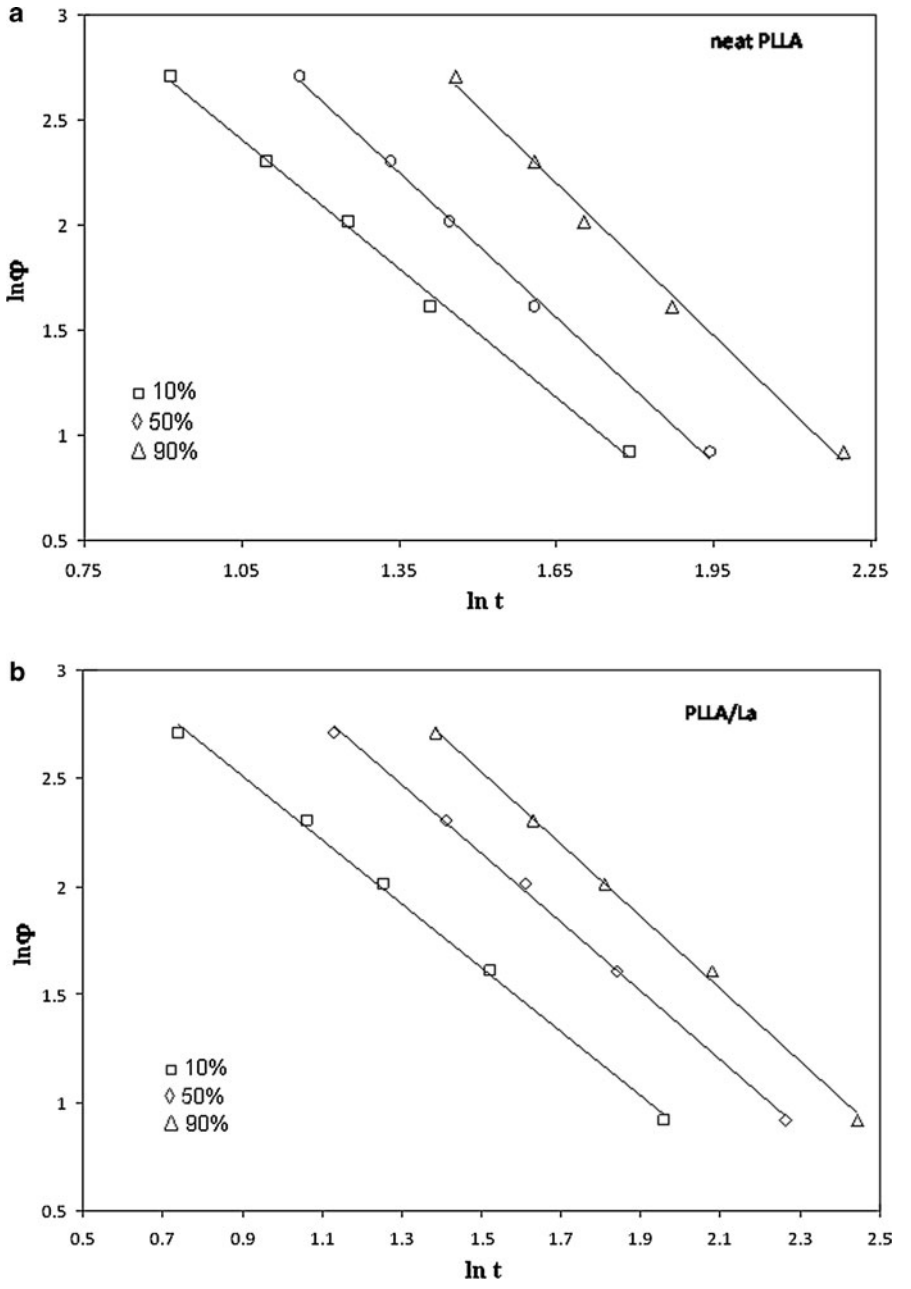

Fig. 7 Plots of $\ln \phi$ versus $\ln t$ from the Mo model for neat PLLA (**a**) and PLLA/La (**b**)

Table 3 The detail of kinetic parameters from Mo model

Sample	$X(t)\%$	α	$F(T)$
PLLA	10	2.05	4.56
	50	2.3	5.36
	90	2.41	6.18
PLLA/La	10	1.48	3.84
	50	1.59	4.54
	90	1.67	5.04

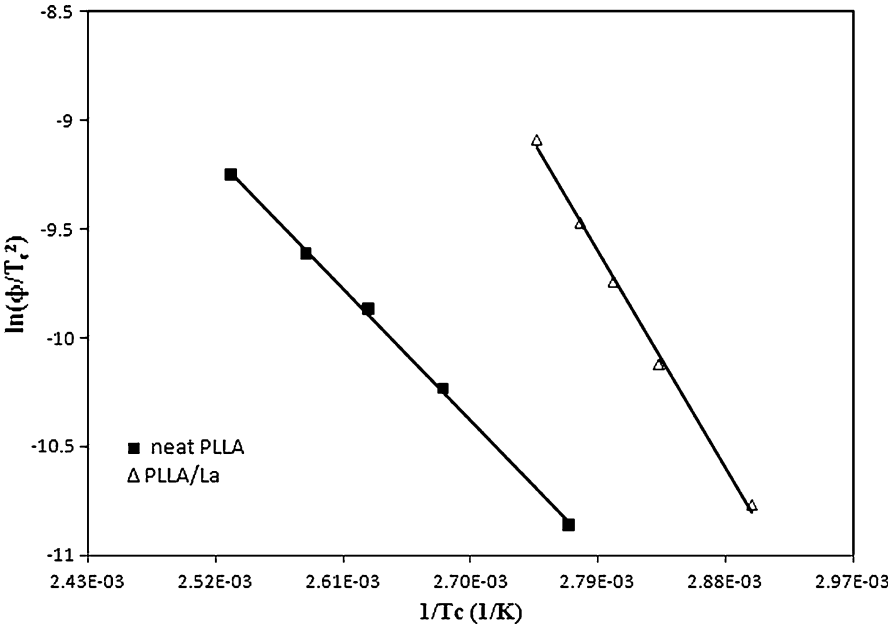

Fig. 8 Kissinger plots of neat PLLA and PLLA/La films

Lauritzen–Hoffman theory

The Lauritzen–Hoffman theory is one of the most important theories on polymer crystallization to explain the crystal growth kinetics. Accordingly, the crystal growth rate (G) of a homopolymer is given by:

$$G = G_0 \exp\left(\frac{-U^*}{R(T_C - T_\infty)}\right) \exp\left(\frac{-K_g}{fT_C\Delta T}\right) \tag{10}$$

where G_0 is a pre-exponent constant; U^* the activation energy for local motion, R the universal gas constant, T_C the crystallization temperature, T_∞ the temperature at which flow ceases and is taken as $T_\infty = T_g - 30K$, ΔT the degree of undercooling ($\Delta T = (T_m^0 - T_C)$, T_m^0 is the equilibrium melting temperature), and f is a factor to

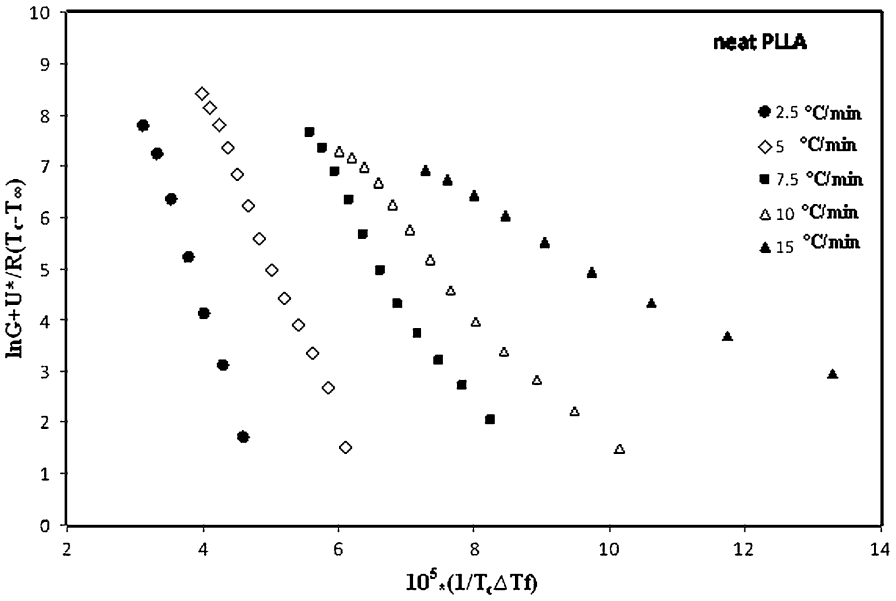

Fig. 9 Lauritzen–Hoffman plots for neat PLLA

account the change of the equilibrium melting enthalpy with temperature, defined as $f = 2T_C/(T_m^0 + T_C)$. K_g is the nucleation constant and defined as:

$$K_g = \frac{nb_0\sigma\sigma_e T_m^0}{k\Delta H_f} \tag{11}$$

where n depends on crystallization regime which is equal to 4 for regimes I and III and 2 in regimes II, b_0 is the molecular thickness, σ and σ_e are the lateral and end surface free energies of the growing crystal, respectively. ΔH_f is the enthalpy of fusion and k is the Boltzmann constant [28]. It can be shown that the spherulite growth rate G can be considered proportional to $(t_{1/2})^{-1}$.

Figure 9 shows the plots of $\ln G + U^*/R(T_C - T_\infty)$ vs. $1/fT_C\Delta T$ for neat PLLA sample at various heating rates, the value of $K_g$can be obtained from the slope. To fit experimental data, $U^* = 6{,}276$ J/mol, $T_m = 479.2$ K and $T_g = 55$ °C were utilized as done in previous studies on PLLA [36]. It has been reported that the transition from regime III to regime II was observed around 115 °C [36]. Thus, it is assumed that all the crystallizations were carried out in regime III under experimental condition in the present work.

The K_g values are used to calculate the fold surface free energy according to Eq. (11). The lateral surface free energy is determined by the Thomas-Stavely equation $\sigma = 0.1\Delta h_f b$. Using the literature values of $\Delta h_f = 1.11 \times 108$ J/m^3 and $b = 0.517$ nm, the values of σ are 15.4×10^{-3} J/m^2 [30]. The values of K_g and σ_e are listed in Table 4.

As shown in Table 4, the values of K_g ranged from 0.69×10^5 to 4.2×10^5 for neat PLLA and 0.55×10^5 to 3.26×10^5 for PLLA/La films. The calculated values

Table 4 Lauritzen–Hoffman parameters for neat PLLA and PLLA/La crystallization

Sample	φ (°C/min)	$10^{-5} \times K_g$ (III) (K^2)	σ_e (erg/cm^2)
PLLA	2.5	4.2	42.15
	5	3.2	32.1
	7.5	2.19	21.98
	10	1.5	15.05
	15	0.69	6.92
PLLA/La	2.5	3.26	32.72
	5	3.25	32.62
	7.5	2	20.07
	10	1.48	14.85
	15	0.55	5.52

of σ_e are from 6.92 to 42.15 for neat PLLA and 5.52 to 32.72 for PLLA/La films under different heating rates. These values are in well agreement with value in other literature [28, 30, 36].

It is found that K_g and σ_e decrease with addition of L-lactide into PLLA matrix, indicating that the presence of L-lactide in PLLA slows down the chain folding barrier, thereby increasing the rate of crystallization of PLLA at heating rate of DSC.

Conclusions

Non-isothermal cold crystallization behavior and kinetics of PLLA and PLLA containing L-lactide dimer have been investigated at various heating rates using DSC. The results revealed that both presence of L-lactide in PLLA and scan rates of DSC influence the cold crystallization process of PLLA. Comparison of the X_C% values of neat PLLA and PLLA/La films at high heating rate leads to the conclusion that the existence of L-lactide obviously affected the crystallization ability. Avrami, Jeziorny and Mo models were found to be suitable and convenient methods to deal with the non-isothermal cold crystallization kinetics of PLLA and PLLA/La. However, Ozawa model was found invalid for describing the crystallization kinetics. The kinetic parameters obtained from these mathematical models such as $t_{1/2}$ and Z_C clearly showed that the addition of L-lactide could enhance the rate of PLLA crystallization. The nucleation parameter was determined by Lauritzen–Hoffman equation. K_g and σ_e are reduced for PLLA/La films compared to neat PLLA suggesting that L-lactide dimer improves crystallization process.

References

1. Liu Y, Wang L, He Y, Fana Zh, Lia S (2010) Non-isothermal crystallization kinetics of poly(L-lactide). Polym Int 59:1616–1621

2. Acar I, Durmus A, Ozgümüs S (2007) Non-isothermal crystallization kinetics and morphology of polyethylene terephthalate modified with polydactic acid. J Appl Polym Sci 106:4180–4191
3. Tsuji H, Miyauchi S (2001) Enzymatic hydrolysis of poly(Lactide)s: effects of molecular weight, L-Lactide content, and enantiomeric and diastereoisomeric polymer blending. Biomacromolecules 2:597–604
4. Li SM, Tenon M, Garreau H, Braud C, Vert M (2000) Enzymatic degradation of stereocopolymers derived from L-DL- and meso-lactides. Polym Degrad Stabil 67:85–90
5. Wang Y, Funari S, Mano J (2006) Influence of semicrystalline morphology on the glass transition of poly(L-lactic acid). Macromol Chem Phys 207:1262–1271
6. Zhi-Hua Zh, Jian-Ming R, Zhong-Cheng Zh, Jian-Peng Z (2007) The kinetics of melting crystallization of poly-L-lactide. Polym Plast Tech Eng 46:863–871
7. Kolstad J (1996) Crystallization kinetics of poly(L-lactide-co-meso-lactide). J Appl Polym Sci 62:1079–1091
8. Zhou WY, Duan B, Wang M, Cheung WL (2009) Crystallization kinetics of poly(L-lactide)/carbonated hydroxyapatite nanocomposite microspheres. J Appl Polym Sci 113:4100–4115
9. Xu H-Sh, Dai XJ, Lamb PR, Li Zh-M (2009) Poly(L-lactide) crystallization induced by multiwall carbon nanotubes at very low loading. J Polym Sci Part B Polym Phys 47:2341–2352
10. Katiyar V, Nanavati H (2011) High molecular weight poly(L-lactic acid) clay nanocomposites via solid-state polymerization. Polym Compos 32:497–509
11. Lu J, Qiu Z, Yang W (2007) Fully biodegradable blends of poly(L-lactide) and poly(ethylene succinate): miscibility, crystallization, and mechanical properties. Polymer 48:4196–4204
12. Tsuji H, Sawada M, Bouapao L (2009) Biodegradable polyesters as crystallization-accelerating agents of poly(L-lactide). ACS Appl Mater Interfaces 1:1719–1730
13. Ohtani Y, Okumura K, Kawaguchi A (2003) Crystallization behavior of amorphous poly(L-lactide). J Macromol Sci Phys 42:875–888
14. Schmidt SC, Hillmyer MA (2001) Polylactide stereocomplex crystallites as nucleating agents for isotactic polylactide. J Polym Sci Part B Polym Phys 39:300–313
15. Baratian S, Hall ES, Lin JS, Xu R, Runt J (2001) Crystallization and solid-state structure of random polylactide copolymers: poly(L-lactide-co-L-lactide)s. Macromolecules 34:4857–4864
16. Wei JC, Sun JR, Wang HJ, Chen XS, Jing XB (2010) Isothermal crystallization behavior and unique banded spherulites of hydroxyapatite/poly(L-lactide) nanocomposites. Chin J Polym Sci (CJPS) 4:499–507
17. Pluta M, Jeszka JK, Boiteux G (2007) Polylactide/montmorillonite nanocomposites: structure, dielectric, viscoelastic and thermal properties. Eur Polym J 43:2819–2835
18. Cao D, Wu L (2009) Poly(L-lactic acid)/silicon dioxide nanocomposite prepared via the in situ melt polycondensation of L-lactic acid in the presence of acidic silica sol: isothermal crystallization and melting behaviors. J Appl Polym Sci 111:1045–1050
19. Sarazin P, Li G, Orts WJ, Favis BD (2008) Binary and ternary blends of polylactide, polycaprolactone and thermoplastic starch. Polymer 49:599–609
20. Nam JY, Okamoto M, Okamoto H, Nakano M, Usuki A, Matsuda M (2006) Morphology and crystallization kinetics in a mixture of low-molecular weight aliphatic amide and polylactide. Polymer 47:1340–1347
21. Hu X, An H, Li ZhM, Geng Y, Li L, Yang Ch (2009) Origin of carbon nanotubes induced poly(L-lactide) crystallization: surface induced conformational order. Macromolecules 42:3215–3218
22. Li Y, Wang Y, Liu L, Han L, Xiang F, Zhou Z (2009) Crystallization improvement of poly(L-lactide) induced by functionalized multiwalled carbon nanotubes. J Polym Sci Part B Polym Phys 47:326–339
23. Zhao Y, Qiu Zh, Yan Sh, Yang W (2011) Crystallization behavior of biodegradable poly(L-lactide)/multiwalled carbon nanotubes nanocomposites from the amorphous state. Polym Eng Sci 51:1564–1573
24. Mobedi H, Mashak A, Nekoomanesh M, Orafai H (2011) L-lactide additive and in vitro degradation performance of poly(L-lactide) films. Iran Polym J 20:237–245
25. Mashak A, Mobedi H, Nekoomanesh M, Ravari F (2011) Crystallization behavior of poly(L-lactide) films in presence of $Mg(OH)_2$ and L-lactide. Iran J Polym Sci Technol (Persian Edition) 23(5):405–413
26. Zilberman M, Schwade ND, Eberhart RC (2004) Protein-loaded bioresorbable fibers and expandable stents: mechanical properties and protein release. J Biomed Mater Res Part B Appl Biomater 69B:1–10

27. Saengsuwan S, Tongkasee P, Sudyoadsuk T, Promarak V, Keawin T, Jungsuttiwong S (2011) Non-isothermal crystallization kinetics and thermal stability of the in situ reinforcing composite films based on thermotropic liquid crystalline polymer and polypropylene. J Therm Anal Calorim 103: 1017–1026
28. Wu D, Wu L, Xu B, Zhang Y, Zhang M (2007) Non-isothermal cold crystallization behavior and kinetics of polylactide/clay nanocomposites. J Polym Sci Part B Polym Phys 45:1100–1113
29. Avrami M (1939) Kinetics of phase change. I general theory. J Chem Phys 7:1103–1112
30. Liao R, Yang B, Yu W, Zhou Ch (2007) Isothermal cold crystallization kinetics of polylactide/nucleating agents. J Appl Polym Sci 104:310–317
31. Jeziorny A (1978) Parameters characterizing the kinetics of the kinetics of the non-isothermal crystallization of poly(ethylene terephthalate) determined by D.S.C. Polymer 19:1142–1144
32. Ozawa T (1971) Kinetics of non- isothermal crystallization. Polymer 12:150–158
33. Liu T, Mo Zh, Wang Sh, Zhang H (1997) Non-isothermal melt and cold crystallization kinetics of poly(aryl ether ether ketone ketone). Polym Eng Sci 37:568–575
34. Qiu Zh, Mo Zh, Yu Y, Zhang H, Sheng Sh, Song C (2000) Non-isothermal melt and cold crystallization kinetics of poly(aryl ether ketone ether ketone ketone). J Appl Polym Sci 77:2865–2871
35. Kissinger HE (1956) Variation of peak temperature with heating rate in differential thermal analysis. J Res Nat Bur Stand 57:217–221
36. Zhou WY, Duan B, Wang M, Cheung WL (2011) Isothermal and nonisothermal crystallization kinetics of poly(L-Lactide)/carbonated hydroxyapatite nanocomposite microspheres. In: Boreddy Reddy (ed) Advances in diverse industrial applications of nanocomposites. ISBN: 978-953-307-202-9, In Tech. http://www.intechopen.com/books/advances-in-diverse-industrial-applications-ofnanocomposites/isothermal-and-non-isothermal-crystallization-kinetics-of-poly-l-lactide-carbonatedhydroxyapatite. Accessed 8 Jan 2012